

# *S-based symplectic tracking with space charge and applications to IOTA*

*Nathan Cook<sup>\*&</sup>, David Bruhwiler<sup>&</sup>, Jonathan Edelen<sup>&</sup>, Chris Hall<sup>&</sup>, Stephen Webb<sup>&</sup>,  
Jeffrey Eldred, Alexander Romanov<sup>#</sup>, Alexander Valishev<sup>#</sup>*



*[\\*ncook@radiasoft.net](mailto:ncook@radiasoft.net)*

*May 9, 2018*

*2018 IOTA/FAST Collaboration Meeting*

*This work is supported the US DOE Office of Science, Office of High Energy Physics: DE-SC0011340.*

# Outline

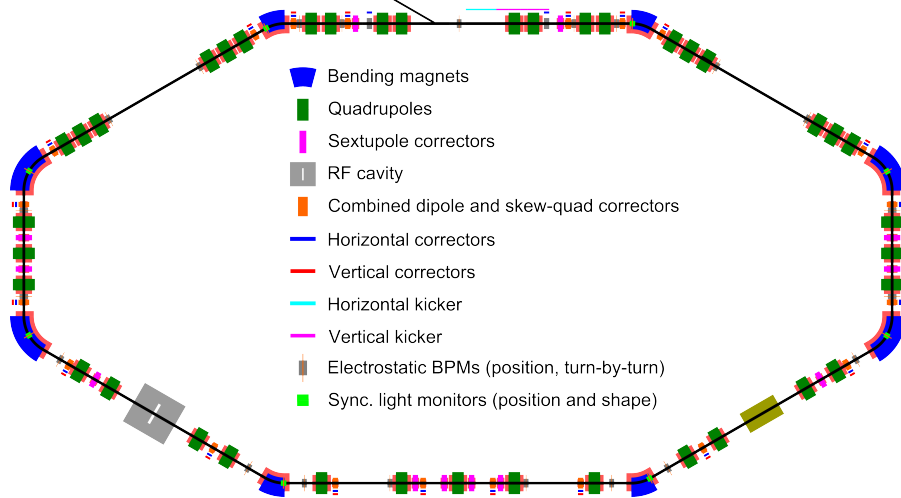
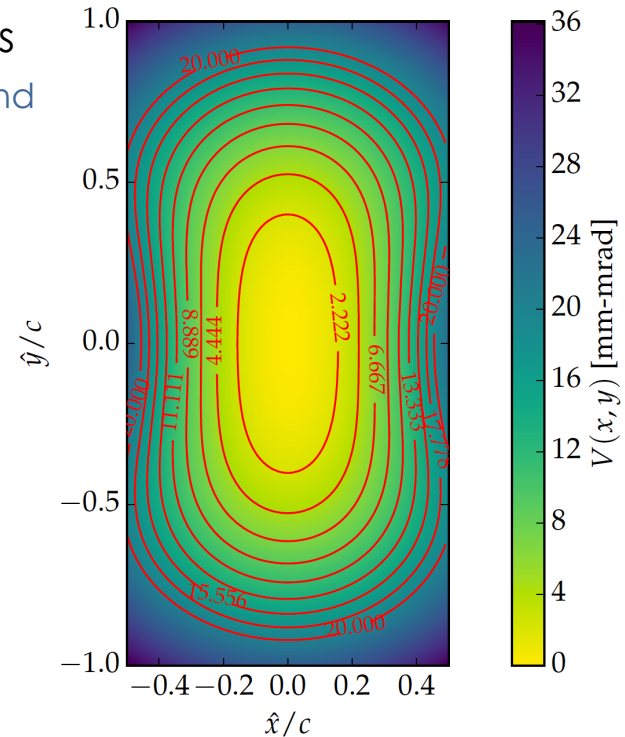
- Motivation - modeling intense beams in IOTA
  - Equilibrium dynamics perturbed by space charge
  - Longterm evolution is critical to nonlinear phenomena (i.e. decoherence)
  - Symplectic, self-consistent tracking presents a solution
- Algorithm - symplectic, s-based, spectral solver
  - Derivation of Hamiltonian and update sequence
  - Corresponding Poisson equation and space charge solve
- Benchmarks and Convergence
  - Example: Expansion in a drift
  - Variations with particle shape and mode number
- Plans for IOTA simulations using Synergia 2.1

# Motivation

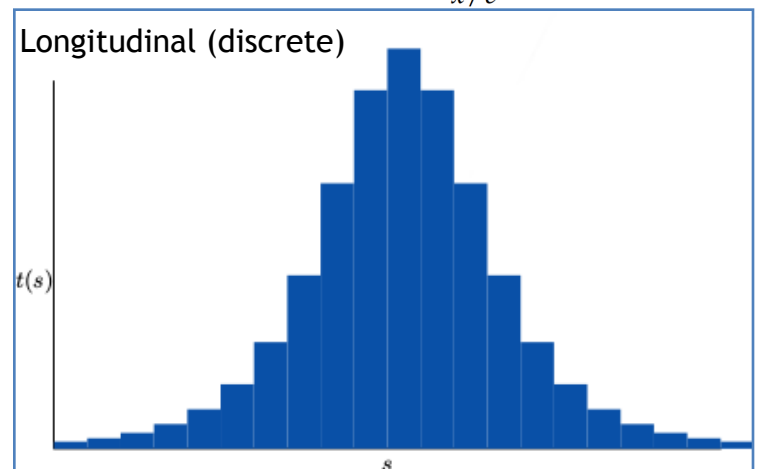
- Meeting community goals requires support for multi-MW hadron beams
  - Scientific and strategic leadership initiative
- High beam power presents significant dynamics challenges
  - Space charge tune shift drives resonance crossings
  - Bunch oscillations drive particles to large amplitudes - e.g. beam halo - and increase losses
    - Machine protection requires  $< 1$  W/m ( $< 0.1\%$  losses)
- Accelerators recoup stability through introducing external (perturbative) nonlinearities
  - I.e. Octupoles generate tune spread with amplitude to damp resonances - nonlinear decoherence
- Most nonlinearities do not preserve regular, periodic motion in the transverse plane! These systems are non-integrable.

# Integrable Optics and the IOTA lattice

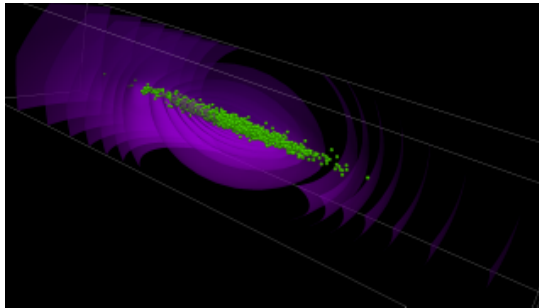
- Experimental initiative to test nonlinear integrable optics
  - Danilov & Nagaitsev “Nonlinear accelerator lattices with one and two analytic invariants,” PRSTAB **13**, 084002 (2010)
- Use of special nonlinear magnet can result in a 2nd invariant of motion, completely integrable dynamics
  - Single particle trajectories are regular and bounded
  - Mitigate parametric resonances via nonlinear decoherence
  - Specific symmetries required:
    - $n\pi$  phase advance between NL inserts
    - $\beta_x(s) = \beta_y(s)$ ,  $D(s)=0$  through underlying drift region
    - Potential is piecewise-constant in  $s$



A. Romanov, “IOTA Optics Update,” presented at *Fast/IOTA Scientific Workshop* (Batavia, June, 2016);



# Beam dynamics and space charge via Synergia 2.1



**Synergia:** A comprehensive accelerator beam dynamics package

<http://web.fnal.gov/sites/synergia/SitePages/Synergia%20Home.aspx>

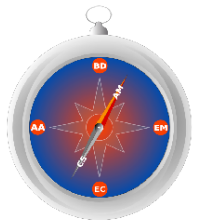
 **Fermilab**  
Accelerator Simulation Group

James Amundson, Qiming Lu, Alexandru Macridin, Leo Michelotti, Chong Shik Park, (Panagiotis Spentzouris), Eric Stern and Timofey Zolkin



Computer time from INCITE

The COMPASS Project  
High Performance Computing for Accelerator Design  
and Optimization  
<https://sharepoint.fnal.gov/sites/compass/SitePages/Home.aspx>



Funded by DOE SciDAC

**CAMPA**

Consortium for Advanced Modeling  
of Particle Accelerators

Funded by DOE

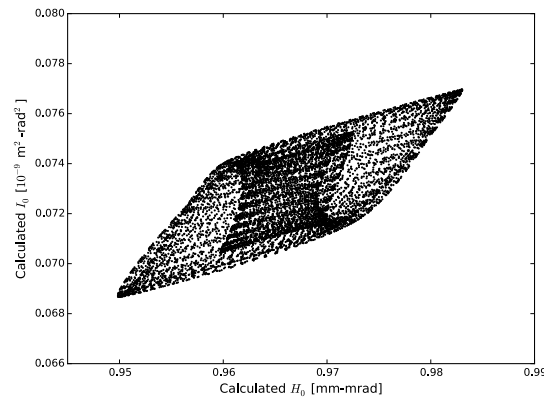


# Longterm single particle simulations

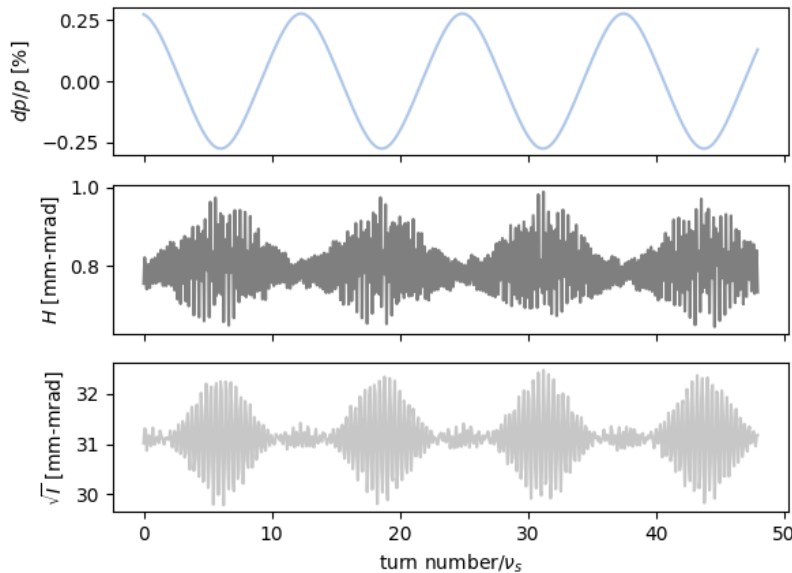
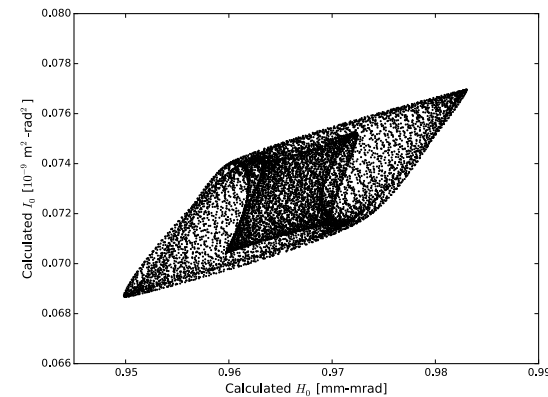
- In zero-current limit, dynamics with idealized lattice are well-behaved on long time scales

- Variations in the invariants are regular and bounded
- Amplitudes of variations scale according to Hamiltonian perturbation analysis

Correlation between 1st and 2nd invariants - 10K turns



Correlation between 1st and 2nd invariants - 100K turns

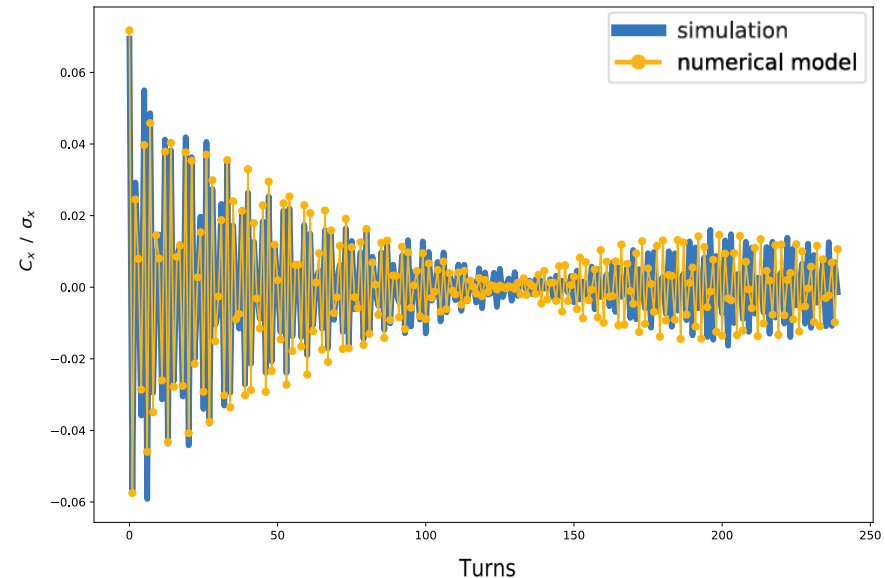
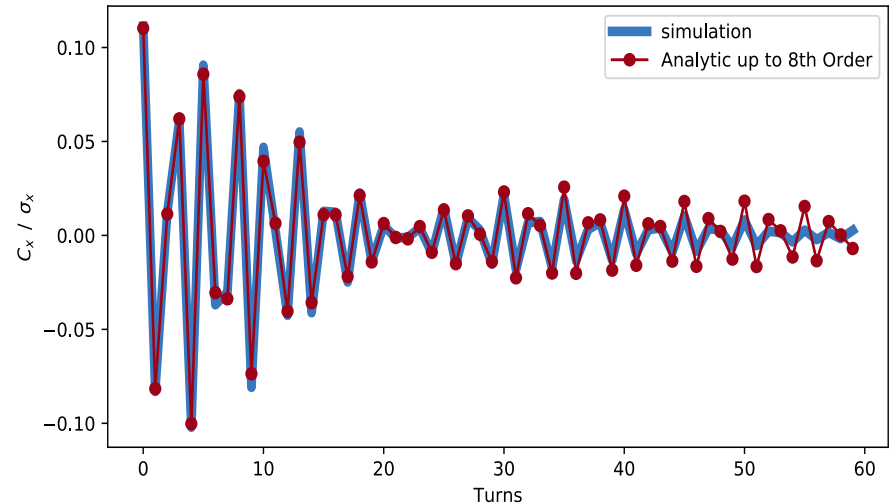


- Initial simulations with RF in an integrable RCS suggest that invariants are well preserved for each super-period of the lattice, modulo the synchrotron frequency
- This workshop: J. Eldred **“Concepts of an RCS for a multi-MW facility at Fermilab”**
- IPAC18: S.D. Webb et al. **“Effects of Synchrotron Motion on Nonlinear Integrable Optics”** THPAF067.

# Nonlinear decoherence persists with space charge

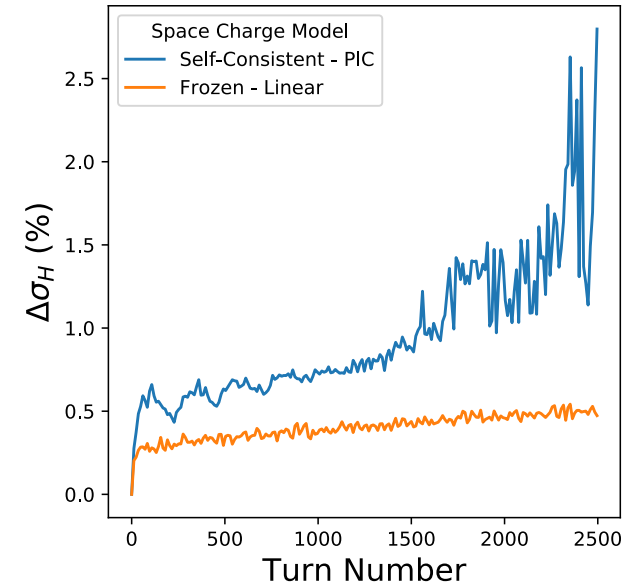
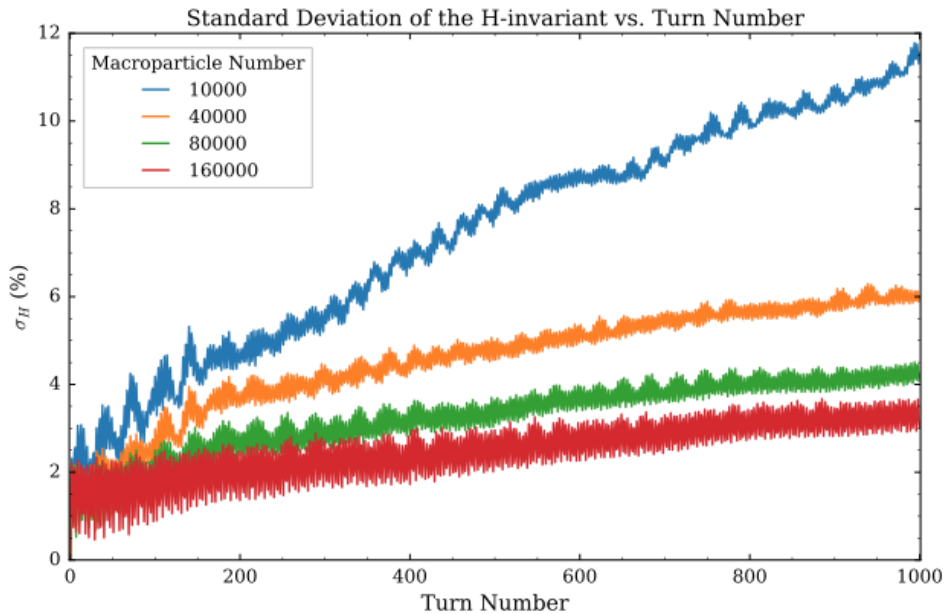
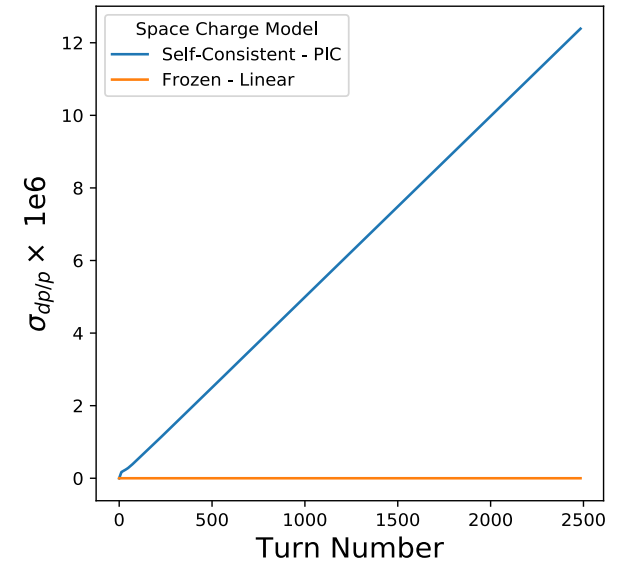
- Decoherence modeling illustrates challenges of incorporating space charge
  - Decoherence damps centroid of offset beam according to NL insert
  - At zero current, rapid damping in agreement with models
  - With space charge, decoherence slows due to feedback, “breathing modes” develop
- Space charge moves beam away from idealized conditions
  - Asymmetric beam yields unequal tunes in each plane
  - Equilibrium distribution is difficult to predict
  - Longterm simulations are required

C.C. Hall IPAC18 THPAK082



# Symplectic algorithms enhance simulation fidelity

- Symplectic algorithms preserve phase space structures
  - Tracking canonical coordinates derived from an approximate Hamiltonian obeys least-action principle
  - Variations from exact solution are bounded, even in the presence of space-charge
- Removal of grid-operations avoids numerical instabilities, e.g. numerical dispersion and grid-heating
  - Analytic propagation reduces high-frequency noise
  - Higher order particle shapes don't necessarily entail higher computational cost





# Recent examples of symplectic PIC

- **S.D. Webb (2016)** : t-based, gridless, electrostatic algorithm
- **J. Qiang (2017)**: t-based electrostatic algorithm with external elements
- **D.T. Abell et al. (2017)**: s-based electromagnetic algorithm with external field coupling and no space-charge
- **Current work**: s-based electrostatic with space-charge - *IPAC 2018 - THPAKK083*

IOP Publishing

Plasma Phys. Control. Fusion 00 (2015) 000000 (9pp)

Plasma Physics and Controlled Fusion

UNCORRECTED PROOF

## A spectral canonical electrostatic algorithm

Stephen D Webb

RadiaSoft, LLC, 1348 Redwood Ave., Boulder CO 80304, USA

E-mail: [swebb@radiasoft.net](mailto:swebb@radiasoft.net)

Received 31 August 2015, revised 23 November 2015

Accepted for publication 7 December 2015

Published



### Abstract

Studying single-particle dynamics over many periods of oscillations is a well-understood problem solved using symplectic integration. Such integration schemes derive their update sequence from an approximate Hamiltonian, guaranteeing that the geometric structure of the underlying problem is preserved. Simulating a self-consistent system over many oscillations can introduce numerical artifacts such as grid heating. This unphysical heating stems from using non-symplectic methods on Hamiltonian systems. With this guidance, we derive an electrostatic algorithm using a discrete form of Hamilton's Principle. The resulting algorithm, a gridless spectral electrostatic macroparticle model, does not exhibit the unphysical heating typical of most particle-in-cell methods. We present results of this using a two-body problem as an example of the algorithm's energy- and momentum-conserving properties.

PHYSICAL REVIEW ACCELERATORS AND BEAMS 20, 014203 (2017)

PHYSICAL REVIEW ACCELERATORS AND BEAMS 20, 052002 (2017)

### Symplectic multiparticle tracking model for self-consistent space-charge simulation

Ji Qiang\*

Lawrence Berkeley National Laboratory, Berkeley, California 94720, USA

(Received 31 August 2016; published 23 January 2017)

Symplectic tracking is important in accelerator beam dynamics simulation. So far, to the best of our knowledge, there is no self-consistent symplectic space-charge tracking model available in the accelerator community. In this paper, we present a two-dimensional and a three-dimensional symplectic multiparticle spectral model for space-charge tracking simulation. This model includes both the effect from external fields and the effect of self-consistent space-charge fields using a split-operator method. Such a model preserves the phase space structure and shows much less numerical emittance growth than the particle-in-cell model in the illustrative examples.

DOI: 10.1103/PhysRevAccelBeams.20.014203

### Symplectic modeling of beam loading in electromagnetic cavities

Dan T. Abell,\* Nathan M. Cook, and Stephen D. Webb

RadiaSoft, LLC, 1348 Redwood Ave., Boulder, Colorado 80304, USA

(Received 3 November 2016; published 22 May 2017)

Simulating beam loading in radio frequency accelerating structures is critical for understanding higher-order mode effects on beam dynamics, such as beam break-up instability in energy recovery linacs. Full wave simulations of beam loading in radio frequency structures are computationally expensive, while reduced models can ignore essential physics and can be difficult to generalize. We present a self-consistent algorithm derived from the least-action principle which can model an arbitrary number of cavity eigenmodes and with a generic beam distribution. It has been implemented in our new Open Library for Investigating Vacuum Electronics (OLIVE).

DOI: 10.1103/PhysRevAccelBeams.20.052002

# Algorithm (1) - Change of Coordinate

- Begin with Electromagnetic Lagrangian (F.E. Low 1958)

$$\mathcal{L} = \int dx_0 dx'_0 \left[ -mc^2 \sqrt{1 - \frac{1}{c^2} \left( \frac{d\mathbf{x}}{dt} \right)^2} - q\phi(\mathbf{x}, t) + \frac{q}{c} \frac{d\mathbf{x}}{dt} \cdot \mathbf{A}(\mathbf{x}, t) \right] f(\mathbf{x}_0, \mathbf{x}'_0) \\ + \frac{1}{8\pi} \int d\mathbf{x} \left[ \left( -\frac{1}{c} \frac{\partial \mathbf{A}}{\partial t} - \nabla \phi \right)^2 - (\nabla \times \mathbf{A})^2 \right].$$

- Transform into s-based coordinate system

$$(x, y, s) \rightarrow (x, y, \xi), \quad \xi = z - \beta_0 ct$$

- Define canonical momentum for coordinate

$$p_\xi = \frac{p_\tau}{\beta_0} = \frac{\gamma mc}{\beta_0}$$

- Valid for  $\beta_0 > 0$
- Note that  $\beta_0$  is a free parameter (but will often be chosen to equate the velocity of the beam in lab frame)

## Algorithm (2) - Simplifying Assumptions

1. The “beam” approximation:  $d\xi/ds \ll 1$

2. No electrostatic elements

- Only scalar potential arises from beam

3. No significant transverse coupling or radiation

$$d\mathbf{x}_{\perp}/ds \cdot \mathbf{A}_{\perp} \approx 0$$

4. No contribution from fringe fields

$$A_s = A_{\text{ext}} + \mathcal{A}$$

With these assumptions, electromagnetic Lagrangian is reduced to:

$$\mathcal{L}_{\text{em}} = \int d\Omega_0 \left[ -\frac{q}{c} \left( \frac{1}{\beta_0} \phi - \mathcal{A} \right) \right] f(\Omega_0) \\ - \frac{1}{8\pi} \int d\mathbf{r}_{\perp} \times \frac{d\xi}{\beta_0 c} \left[ \left( \beta_0 \frac{\partial \mathcal{A}}{\partial \xi} - \frac{\partial \phi}{\partial \xi} \right)^2 + (\nabla_{\perp} \phi)^2 - (\nabla_{\perp} \mathcal{A})^2 \right]$$

## Algorithm (3) - Obtaining the potential

- This Lagrangian is degenerate with respect to the fields (i.e. there is no canonical momentum for  $\phi$ )
- We can use the Euler-Lagrange equations to obtain an auxiliary condition:

$$\partial_\mu \frac{\partial \mathcal{L}}{\partial(\partial_\mu \phi)} - \frac{\partial \mathcal{L}}{\partial \phi} = 0 \qquad \partial_\mu \frac{\partial \mathcal{L}}{\partial(\partial_\mu \mathcal{A})} - \frac{\partial \mathcal{L}}{\partial \mathcal{A}} = 0$$

- We combine these equations to yield a single constraint describing the pseudopotential  $\psi$ :

$$\psi = \beta_0 \mathcal{A} - \phi \qquad \left( \frac{1}{\gamma_0^2} \partial_\xi^2 + \nabla_\perp^2 \right) \psi = \frac{4\pi q}{\gamma_0^2} n(\xi, x_\perp)$$

- In 2D, we ignore the  $\xi$  term
- Note that the total force scales with  $1/\gamma_0^2$
- For  $\gamma_0 \gg 1$ , the force is transverse

# Algorithm (4) - Hamiltonian and Update Sequence

- The Hamiltonian for the system is:

$$\mathcal{H} = \sum_j -\sqrt{\left(\beta_0 p_j^{(\xi)}\right)^2 - \left(\mathbf{p}_j^{(\perp)}\right)^2 - (w_j mc)^2} + p_j^{(\xi)} - \frac{w_j q}{\beta_0 c} \psi$$

- Particle coordinates update via Hamilton's equations:

$$\mathbf{x}_\perp = \mathbf{x}_\perp^0 + \frac{\mathbf{p}^{(\perp)}}{\sqrt{\left(\beta_0 p^{(\xi)}\right)^2 - \left(\mathbf{p}^{(\perp)}\right)^2 - (wmc)^2}} \Delta s$$

- No additional kick without external potential

- Complete update follows splitting method:

$$\mathcal{M}(h) \approx \mathcal{M}_{\text{drift}}(h/2) \mathcal{M}_{\text{ext}}(h/2) \mathcal{M}_{\text{sc}}(h) \mathcal{M}_{\text{ext}}(h/2) \mathcal{M}_{\text{drift}}(h/2)$$

- Obtain second order accuracy in h for particle update

# Particle and field representations

- We describe our fields using an orthonormal Fourier basis:

$$\psi = \frac{1}{\sqrt{L_x L_y}} \sum_{k_x, k_y} e^{ik_x x} e^{ik_y y} \sigma_{k_x, k_y}$$

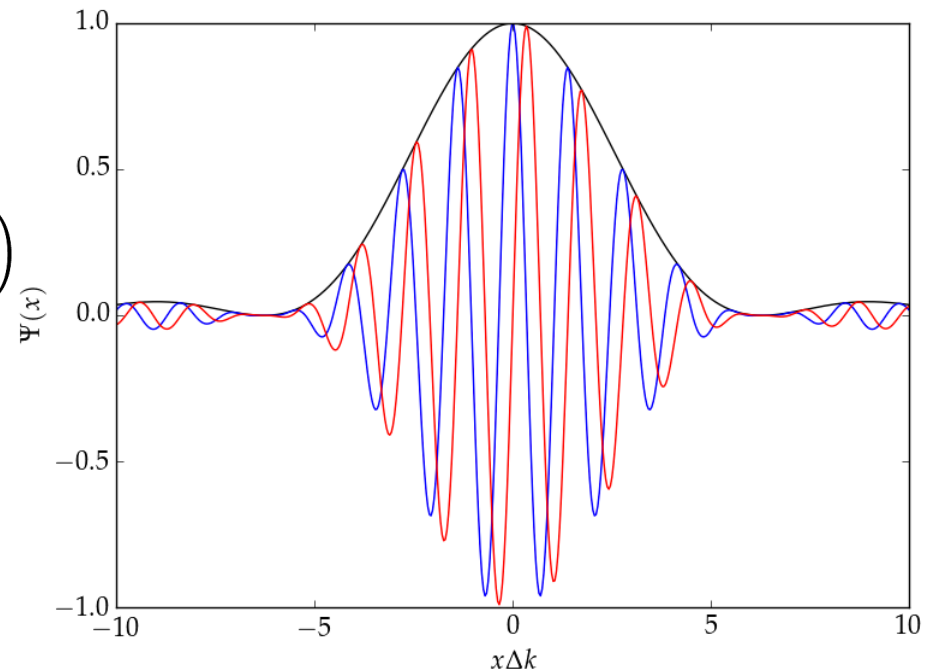
- where  $k_{x,y} = 2\pi n / L_{x,y}$  for  $n \in [-N \dots N]$
- $\sigma_{k_x, k_y}$  represents the normalized amplitude of each mode

- Define macroparticles with delta-functions in  $\mathbf{p}$  and shapes in  $\mathbf{x}$ :

$$\Psi(\mathbf{r}, \mathbf{p}) = \sum_{j=1}^{N_{\text{macro}}} w_j \Lambda(\mathbf{r} - \mathbf{r}^{(j)}) \delta(\mathbf{p} - \mathbf{p}^{(j)})$$

- delta- and tent-functions are used in these examples
- Tent is smooth in k-space

$$\tilde{\Lambda}(\mathbf{k}) = \left( \frac{\sin\left(\frac{\mathbf{k}\Delta x}{2\pi}\right)}{\frac{\mathbf{k}\Delta x}{2\pi}} \right)^2$$



# Field solve operation

- Field solve requires computation of particle contributions to  $\sigma_{\mathbf{k}}$

$$\sigma_{\mathbf{k}} \propto \frac{1}{L_x L_y} \sum_j \Lambda(\tilde{\mathbf{k}}) \frac{e^{i\mathbf{k} \cdot \mathbf{x}^\perp}}{\mathcal{K}}$$

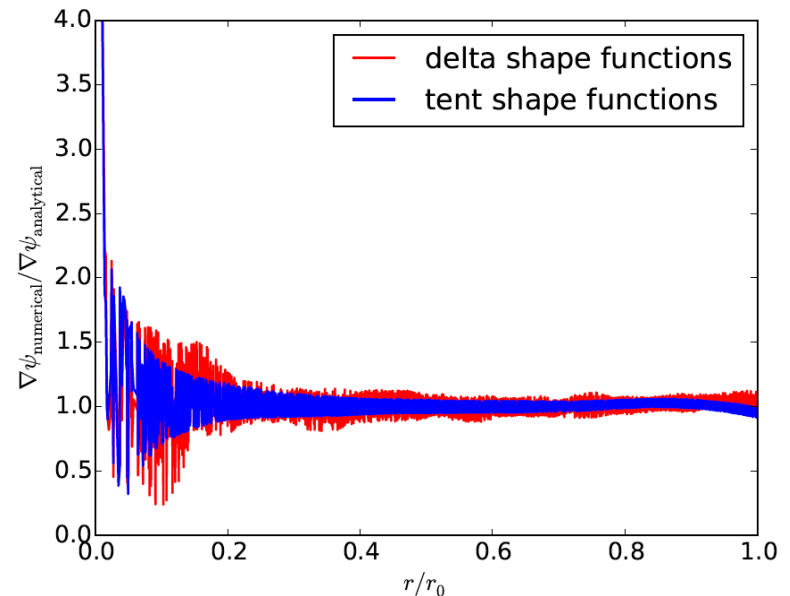
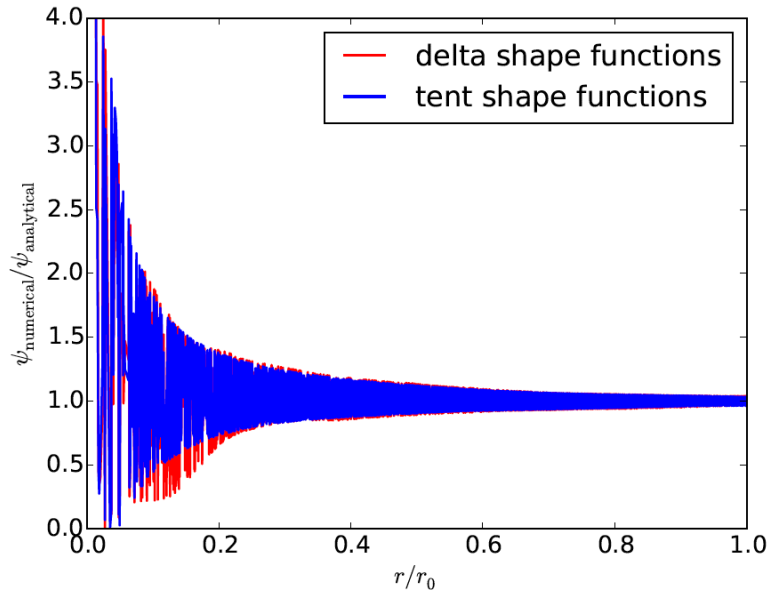
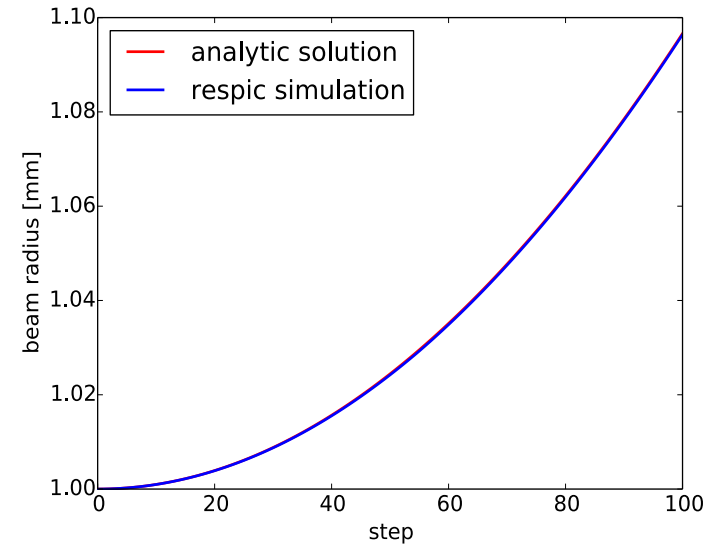
$$\tilde{\Lambda}(\mathbf{k}) = \frac{1}{\sqrt{2\pi}^D} \int d\mathbf{x} e^{-i\mathbf{k} \cdot \mathbf{x}} \Lambda(\mathbf{x})$$

$$\mathcal{K}_{m,n} = k_m^2 k_n^2$$

- Computes  $m \times n$  amplitudes
- Kick analytically computes  $\nabla\psi$
- Field solve is global and gridless
  - Removes load balancing concerns stemming from local decomposition
  - Global exchange can limit scalability beyond ~10,000 cores
    - See H. Vincenti and J-L Vay, **Comp. Phys. Comm.**, **200**, 147-167 (2016)
- Solver admits arbitrary choice of shape
  - Functions complexity in Fourier space matters
    - Gaussian  $\leftrightarrow$  Gaussian, Square  $\leftrightarrow$  Sinc
  - Broadband spatial distributions may be no more difficult to compute in Fourier space than narrow distributions
    - Eliminates polynomial scaling of arbitrary order FDTD stencils

# Benchmarks - Expansion in a drift

- A simple benchmark: K-V beam expanding in a drift
  - Initially zero transverse momentum
  - Excellent agreement with analytic solution
  - Tent-shape function shows improved kick fidelity, especially at low radii where  $\nabla\psi \rightarrow 0$





# Future Work

- Implementation of solver within Synergia
  - Improved particle shapes
  - Parallelization within Synergia MPI framework
  - Further benchmarking for speed and convergence
- Long-term tracking with space charge
  - Decoherence and beam mismatch within IOTA
  - Stability within an integrable RCS
- Wake effects in IOTA
  - Evaluate wake function within same basis and develop corresponding Hamiltonian update sequence
- Cloud-based Synergia simulations with choice of solver and IOTA lattices
  - <https://beta.sirepo.com/>

# Cloud-based Synergia simulations of IOTA

- Support for lattice construction/import, lattice functions, tune and chromaticity adjustments, bunch matching, and visualization
- Execute simulations with different space charge solvers (frozen model, 2D, 3D, symplectic) and tracking modes (direct symplectic, polynomial maps)
- Browser-based GUI running on Docker application container
- Share with URL, or export self-contained Python executable

The screenshot displays the Synergia web interface for the IOTA machine. It is divided into several panels:

- Beamline Report - machine:** Shows a circular beamline layout with various elements represented by colored rectangles and triangles. A 1m scale bar is provided.
- Beamline Editor - machine:** A drag-and-drop interface for defining the beamline, containing buttons for various element types such as oA, bpm, QA1R, oA1, QA2R, oA2, bpm, QASR, oA3, QAR, obm, D1R, BR\_Line, D2R, CR\_Line, DSR, DR\_Line, DDr, E\_Line, D1L, DL\_Line, DSL, CL\_line, DSL, BL\_Line, D1L, obm, QAL, oA3, QASL, bpm, oA2, QA2L, oA1, QA1L, bpm, and oA.
- Beamlines:** A table listing beamline elements with their descriptions, number of elements, start-end positions, lengths, and bends.
- Beamline Elements:** A table listing individual beamline elements with their descriptions, lengths, and bends.
- Bunch:** A configuration panel for the bunch, including particle type (Proton), momentum (0.0685 GeV), horizontal and vertical emittances (3.9e-6 m-rad), longitudinal bunch size (0.0673 m), Delta-p/p spread (0.001), number of real particles (1.5e+8), number of macro particles (5e+4), pseudorandom number generator seed (1.415926e+6), and space between bunches (0.0673).
- Bunch Report:** A 2D histogram showing the distribution of particles in the x-y plane (x and y in mm), with a color scale from 0 to 24.

# Conclusions

- The IOTA ring will support an experimental program for novel nonlinear dynamics and intense beam studies
  - At these intensities, longterm studies are needed for analysis of beam equilibria, nonlinear decoherence, and integrability
  - Traditional methods may be insufficient to model these systems with high fidelity, but symplectic algorithms offer a solution
- We have demonstrated an S-based algorithm for symplectic, self-consistent tracking
  - A spectral field decomposition permits high-order particle shapes
  - Gridless implementation eliminates numerical noise, unphysical heating, and propagation instabilities
- The solver will be added to the Synergia framework for fully symplectic, parallel simulations
  - Support IOTA and integrable RCS designs
- We plan to extend this approach to incorporate wake functions for additional IOTA studies

***Thanks for listening!***

*This work is supported the US DOE Office of Science, Office of High Energy Physics: DE-SC0011340.*

# (Semi)Analytical model for decoherence

- Consider a bunch of particles with amplitude-dependent tune spread given by

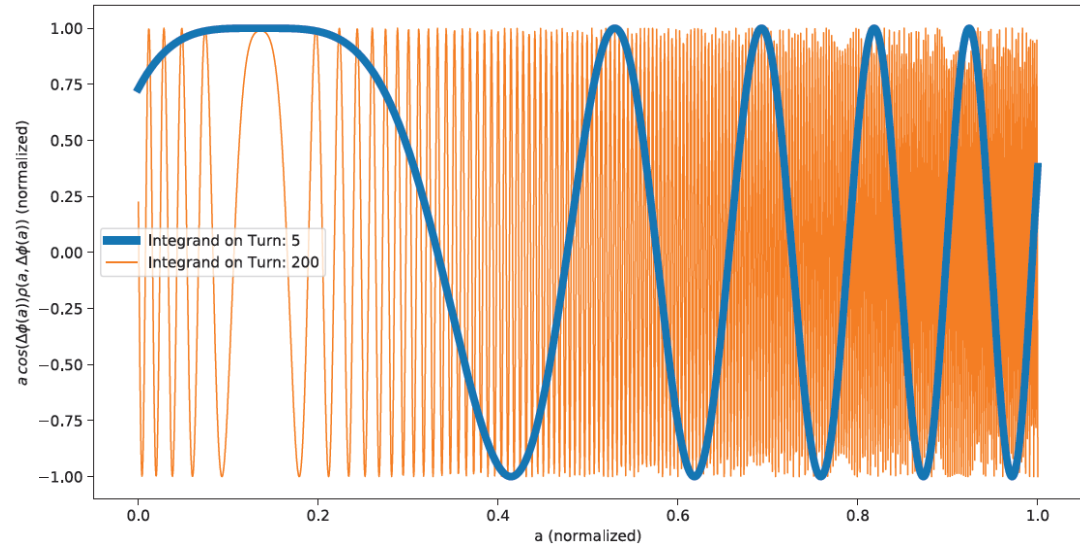
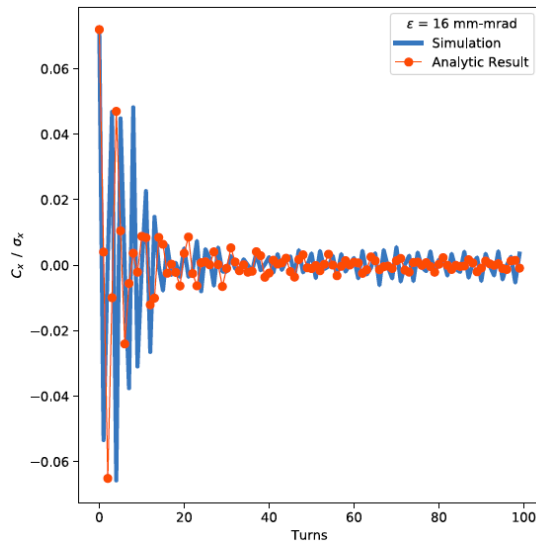
$$\nu = \nu_0 - \sum_{i=1} \mu_i a^{2i}$$

R.E. Meller et al. SSC-N-360, 1987

- The evolution of the bunch centroid, if offset by an initial position, is given by:

$$\bar{x}(N) = \sigma_x \int_0^\infty da \int_0^{2\pi} d\varphi \arccos(\varphi) \rho(a, \varphi - 2\pi N\nu)$$

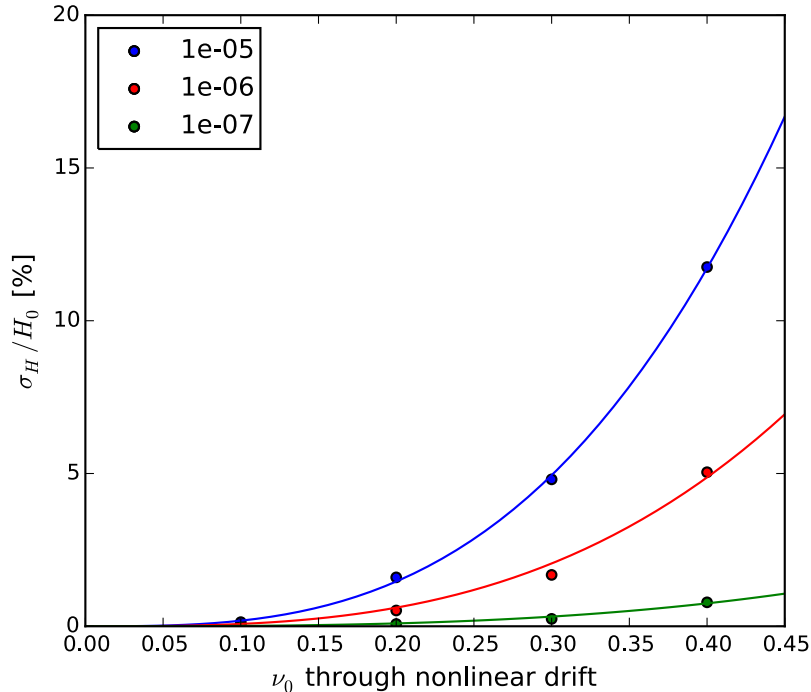
- For a waterbag distribution, this integral is difficult to solve (lower right) beyond octupolar contribution, which provides a poor fit (lower left)



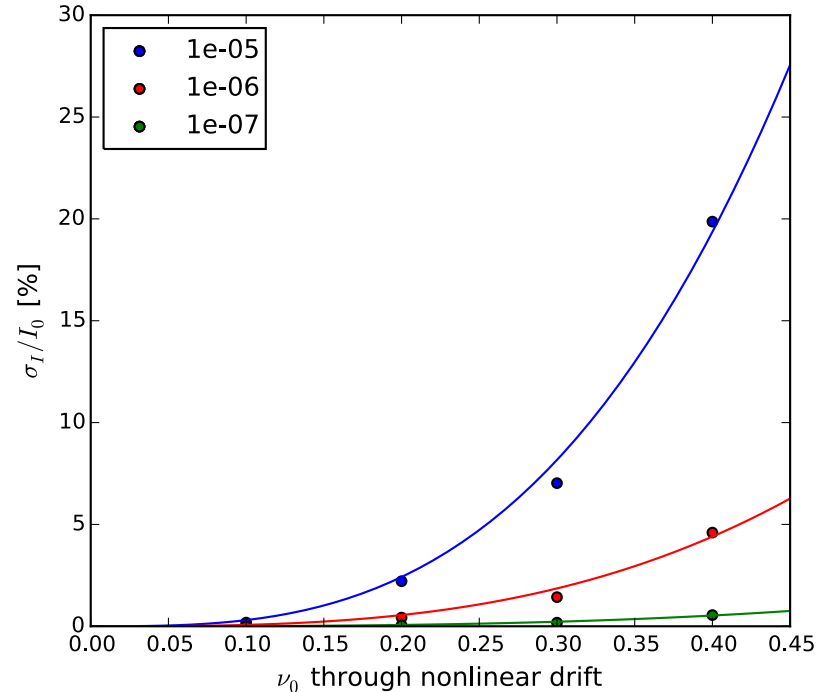
# Variation in the first invariant - $H_0$

- Simulated a toy-model IOTA lattice, comprised of a nonlinear element followed by a corresponding  $6 \times 6$  matrix representing a thin double-focusing lens.
  - Variations of the nonlinear element with different  $\nu_0$  are calculated and scaled using a MADX script

Standard Deviation in H versus phase advance  $\nu_0$

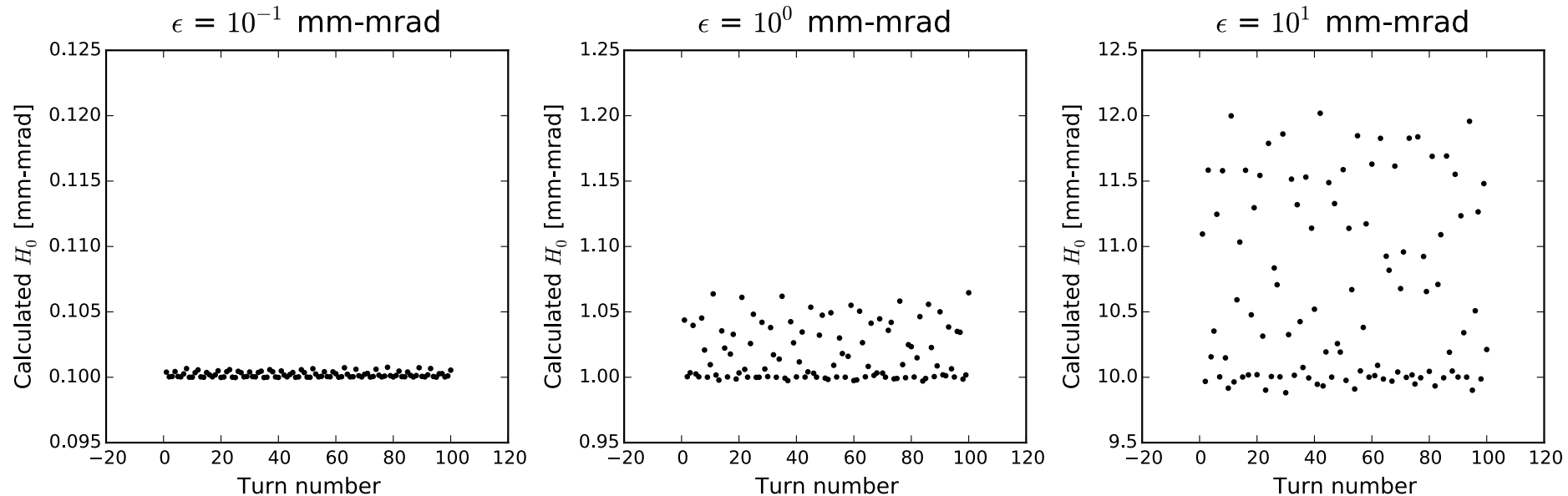


Standard Deviation in I versus phase advance  $\nu_0$



# Variation in $H_0$ with increasing emittance

- Greater variation in  $H_0$  with increasing emittance — coefficients in the expansion of the Hamiltonian vary with  $\epsilon^3$ .

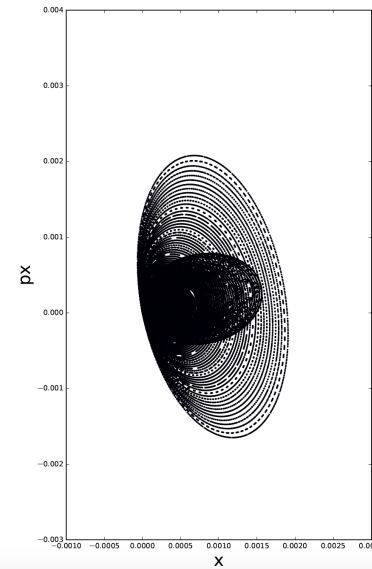


- i.e. For a NL segment with  $\nu_0 = 0.3$ , a KV distribution with  $H_0 = 10$  mm-mrad demonstrates an average r.m.s. variation of 5% in calculated value of  $H_0$ .

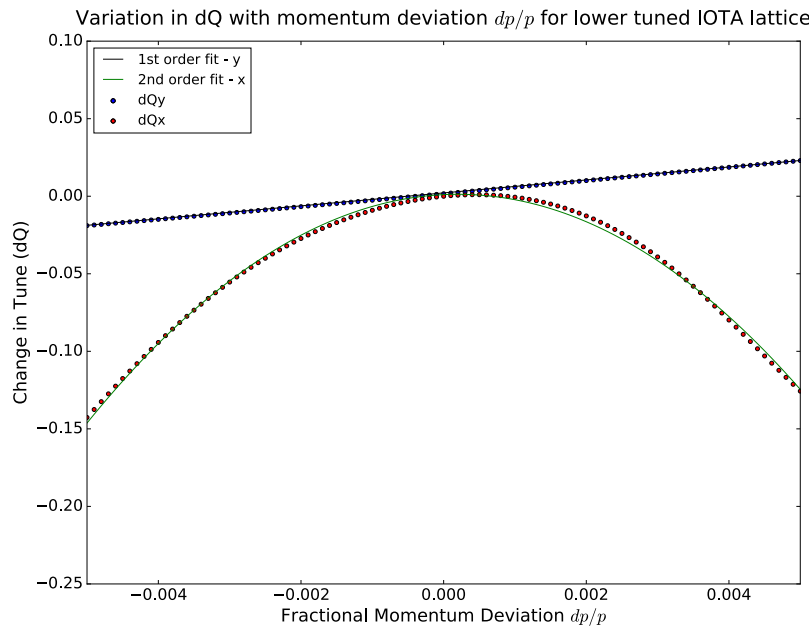
# Nonlinear chromaticity, dispersion in IOTA

- IOTA is a small ring with tight focusing.
  - Large phase advance yields large natural chromaticity
  - Dipole nonlinearities contribute significantly to focusing, further nonlinear chromatic effects
- Nonlinear dispersion complicates chromaticity correction

x-px for 500 turns for lattice Lower Tune IOTA 8-2



A single turn around IOTA with varying  $\delta p$  illustrates nonlinear dispersion.



x displacement after one turn versus momentum offset

